ELSEVIER

Cardiovascular Research 69 (2006) 423 – 431

Cardiovascular Research

www.elsevier.com/locate/cardiores

Structural, functional and metabolic remodeling of rat left ventricular myocytes in normal and in sodium-supplemented pregnancy

V. Bassien-Capsa [a], J.-C. Fouron [a,b], B. Comte [a,c], A. Chorvatova [a,b,*]

[a] *Research Center, Sainte-Justine Hospital, Canada*
[b] *Department of Pediatrics, University of Montreal, Canada*
[c] *Department of Nutrition, University of Montreal, Canada*

Received 10 May 2005; received in revised form 24 October 2005; accepted 31 October 2005
Available online 7 December 2005
Time for primary review 27 days

Abstract

Objectives: Pregnancy is an important physiological condition associated with hemodynamic and endocrine changes that affect the heart. Nevertheless, very little is known about cardiomyocyte remodeling in this condition. Here, we studied the morphological, functional and metabolic remodeling of rat left ventricular myocytes that occurs in late stages of normal pregnancy (P) and in experimental preeclampsia induced by elevated (0.9%) sodium intake (P0.9).

Methods: We applied confocal microscopy to examine the morphology and the contractility of single cells, while the patch clamp technique was used to assay ionic currents.

Results: Our results revealed a significant increase in the volume of single left ventricular cardiac myocytes in P, mainly resulting from cell elongation. In P0.9, further increase in the cell length led to a significant rise in the length/width ratio. Cell contractility was significantly decreased in glucose-based solutions in response to stimulation at 0.5 Hz and 6 Hz in P as well as in P0.9. The density of L-type calcium current ($I_{Ca}L$) was not significantly altered in P or in P0.9. Metabolic substrates lactate and pyruvate, increased in the blood of P and P0.9 rats, enhanced contractility in P, without affecting $I_{Ca}L$. The same effect, present but blunted in P0.9, was associated with a significant increase in $I_{Ca}L$.

Conclusion: Our results demonstrate that processes of adaptive remodeling take place in normal pregnancy, while maladaptive components are identified in experimental preeclampsia; they also reveal an adaptation in the use of energy substrates in pregnancy and its impairment by sodium supplementation.

Keywords: L-type calcium current; Cardiomyocytes; Metabolism; Pregnancy; Hypertension

1. Introduction

Pregnancy induces significant adaptations in the cardiovascular system, associated with hemodynamic and endocrine changes that contribute to maternal volume expansion and are necessary for fetal homeostasis, development and well-being [1]. Systemic arterial vasodilatation represents one of the first detectable changes in hemodynamics that initiates a cascade of compensations in the circulation and volume homeostasis that also affect the heart: cardiac output rises in response to increase in the heart rate and achieves its greatest value in the final stages of delivery, placing an enhanced volume load on the heart. Blood volume expansion leads to adaptations of the myocardium that affect mainly the left ventricle (LV), more susceptible to increased load. In contrast to pathological conditions, these alterations are associated with physiological reduction of blood pressure (BP) and are reversible. The natural volume

* Corresponding author. Research Center of Sainte Justine Hospital, 3175 Cote Sainte Catherine, H3T 1C5 Montreal, Canada. Tel.: +1 514 345 4931x4366; fax: +1 514 345 4801.
E-mail address: alzbeta.chorvatova@recherche-ste-justine.qc.ca (A. Chorvatova).

0008-6363/$ - see front matter © 2005 European Society of Cardiology. Published by Elsevier B.V. All rights reserved.
doi:10.1016/j.cardiores.2005.10.017

overload in pregnancy is frequently associated with increase in LV size and mass, leading to LV hypertrophy (LVH) [2–4].

The most important pathology during pregnancy is hypertension [5], in particular preeclampsia, affecting 6 to 10% of all pregnancies. In this condition, instead of decreasing, BP is significantly increased, producing an acute pressure overload on left ventricle [6,7]. For long, duration of the disease was thought to be too brief to induce structural cardiac changes. However, in recent years, studies of gestational hypertension identified changes in LV geometry as an important risk factor [8–10], correlating with increase in fetal and maternal mortality and morbidity. To date, very little information is available on structure/function modifications at the single cardiomyocyte level.

This study examined whether left ventricular cardiomyocytes undergo structural, functional and metabolic remodeling in normal pregnancy in rat and whether this remodeling is altered by sodium supplementation. To investigate cardiomyocyte remodeling during pregnancy, a rat model was chosen due to close resemblances between pregnancies in rats [11,12] and in humans [13]. A condition comparable to preeclampsia was induced experimentally by sodium supplementation, in regard to a recent work that showed that an increase in the dietary NaCl in the last week of pregnancy induced alterations similar to preeclampsia [14], including higher BP and significantly and durably attenuated renin–angiotensin–aldosterone system [15].

2. Materials and methods

2.1. Animals and cardiomyocyte isolation

Female Sprague–Dawley rats (13–14 weeks old, Charles River, Canada) received a 0.9% NaCl supplement in tap water for the last 7 days of pregnancy [14,15]. Two groups of age-matched pregnant and never pregnant rats were also used. Rats were killed at the 21st day of pregnancy by decapitation. All procedures were performed in accordance with the NIH and the Canadian Council for the Protection of Animals (CCPA) guidelines. Left ventricular myocytes were isolated following retrograde perfusion of the heart with proteolytic enzymes [16]. Myocytes were maintained in a storage solution at 4 °C until used. Only cells showing clearly defined striations were used in up to 10 h following isolation.

2.2. Whole heart echocardiography

Echocardiography was performed on isoflurane (2%/L of O_2/min)-anesthetized rats using a 128XP/10c instrument from Acuston (Mountain View, U.S.A.) equipped with a 7 MHz transducer. LV shortening fraction was calculated as (diastolic − systolic)/diastolic dimensions.

2.3. Confocal microscopy

To label sarcolemma and t-tubule system, myocytes were stained with lipophilic membrane fluorescent probe di-8-ANEPPS (5 μmol/L for 5 min at room temperature) [17]. 3D images were taken by inverted laser scanning confocal microscope LSM 510 (Zeiss, core lab of Sainte-Justine Research Center; PlanNeofluar 63×/1.3 oil, 488 nm Ar/ion, LP 505) and recorded by averaging four lines using 1.2 μm steps in the z-stack (pinhole opening of 417 μm, scaling 0.16 μm × 0.16 μm). Sarcomere length was determined in each cell as a mean length of at least three sarcomeres. For length and width data, some measurements obtained from transmission images were also added. Fluorescent probe Tetramethylrhodamine TMRM (10 nmol/L for 10 min at room temperature) was used to image mitochondria (543 nm He/Ne, LP 560 nm, pinhole opening 106 μm, scaling 0.2 μm × 0.2 μm). At least three measurements were averaged in each cell.

Rapid line-scan confocal imaging was used to record contractions. Cells were field-stimulated to contract using Pt electrodes, operated by a pulse generator (DS-2A, Digitimer Ltd., U.S.A.) and by a trigger generator (DG-2, Digitimer Ltd., U.S.A.) under external perfusion at 35±1 °C. Maximum contraction was calculated as a percentage of Δ cell length=(length-maximal shortening)/length. Only cells with two contracting edges were taken into consideration.

2.4. Electrophysiology

Myocytes were voltage clamped using the Axopatch 200B patch clamp amplifier linked to a Digidata 1200B A/D interface. Currents were acquired using Clampex 9 and analyzed with Clampfit 9 from pClamp package (Axon Instruments, USA). Micropipettes were fabricated from filamented borosilicate glass GC150TF (Harvard, Canada) using pipette pooler (PP-830, Narishige, Japan) and polisher (MF-830, Narishige, Japan) to give tip resistances of 1 MΩ when filled with standard physiological solution (in mmol/L: CsCl, 130.0; $CaCl_2$, 1.0; NaCl, 10.0; HEPES, 10.0 adjusted to pH 7.25 with CsOH). Cells were pre-incubated in the presence of BAPTA-AM (10 μmol/L for 15 min) prior to patch clamp experiments. Membrane currents were measured by the perforated patch clamp method using Amphotericin B (240–480 μg/mL) as the pore-forming agent. All measurements were undertaken at 35±1 °C.

2.5. Blood analyses

Blood was collected immediately after decapitation. The samples were processed within 24 h and determined by standard enzymatic methods [18]. For pyruvate measurement, blood sample was treated with 5% trichloroacetic acid and immediately vortexed for 2 min. Each sample was then centrifuged for 4 min at 10,000×g, the supernatant collected and promptly frozen at −20 °C. Pyruvate was subsequently determined by standard enzymatic dosage. The dosages

were performed by the Clinical Biochemistry Lab at Sainte-Justine Hospital.

2.6. Solutions and drugs

The storage solution contained (in mmol/L): NaCl, 130.0; KCl, 5.4; $MgCl_2 \cdot 6H_2O$, 1.4; NaH_2PO_4, 0.4; creatine, 10.0; taurine, 20.0; glucose, 10.0; and HEPES, 10.0; titrated to pH 7.30 with NaOH. Basic external solution contained (in mmol/L): NaCl, 140.0; KCl, 5.4; $CaCl_2$, 2.0; $MgCl_2$, 1.0; glucose, 10.0; HEPES, 10.0; adjusted to pH 7.35 with NaOH. CsCl (5 mmol/L) was added to this solution for $I_{Ca}L$ measurements. Pyruvate was prepared freshly, while lactate and octanoate were each added to the basic external solution from the 100 mmol/L stock-solution where pH was carefully adjusted to 7.2. Final concentrations of 100 μmol/L for pyruvate, 1 mmol/L for lactate and 1 mmol/L for octanoate were used. All chemicals were from Sigma (Canada), whereas fluorescent probes (di-8-ANEPPS and TMRM) were from Molecular Probes (U.S.A.).

2.7. Data analysis

Data are shown as mean±standard error (S.E.M.). Comparison between means was made using one-way analysis of variance (ANOVA), followed by Bonferroni post-tests, except for $I_{Ca}L$ where Tukey post-tests were used. Data from at least five different animals were taken in each condition before comparison.

3. Results

3.1. Whole heart parameters

First, to evaluate cardiac changes during pregnancy, whole-heart parameters were determined. Animal weights were established together with weights of placenta and number of offspring in pregnant rats (Table 1A). Data from healthy pregnant rats (P) were compared to age-matched non-pregnant females (NP), while pregnant rats receiving 0.9% NaCl supplement (P0.9) were related to P. When the weight of placenta was excluded from the total weight of pregnant rats (P or P0.9), the resulting body weights were not significantly different from NP. Both wet heart weights (WHWs) and dry HWs (DHWs) were compared. Surprisingly, we observed a decrease in WHW in P, leading to a significant decrease of the WHW/DHW ratio. In P0.9, WHW was significantly increased when compared to P and this result was translated into an increase in WHW/DHW ratio. However, the WHW in P0.9 remained unchanged when compared to NP. DHWs were identical in all studied conditions. Sodium supplementation given to non-pregnant rats (NP0.9) did not affect WHW or DHW compared to NP (data not shown).

Echocardiography data (Table 1B), obtained from M-mode tracings (Fig. 1A), revealed significant increase in the LV wall thickness in P, without further changes in P0.9. LV dimensions of the heart were not significantly modified. The shortening fraction was significantly increased in P0.9; no significant change was identified in P. Heart rate (302±13 beats/min (BPM) (n=6) in NP) had an increasing tendency in P (320±12 BPM (n=6)) and in P0.9 (330±11 BPM (n=11)). Recorded values were somewhat lower than previously identified [19], possibly a consequence of anesthesia. BP (120–125 mm Hg in NP and in P0.9) was decreased in P (105–110 mm Hg), as published previously [15].

3.2. Cardiomyocyte morphology

Morphology of single LV myocytes was analyzed from 3D confocal images of non-contracting cells stained with membrane probe di-8-ANEPPS (Fig. 1Ba). Table 2 summa-

Table 1
Whole heart parameters

A) Parameter	Unit	ABB	NP	P	P0.9
Total weight	g	BW	N.A.	357.9±4.2 (17)	363.4±3.5 (21)
Placenta weight	g		N.A.	78.0±2.1 (17)	75.3±2.9 (21)
Number of fetuses			N.A.	13±1 (17)	13±1 (21)
Body weight	g		285.3±4.3 (19)	279.9±3.8 (17)	288.2±2.7 (21)
Wet heart weight	mg	WHW	880.7±18.3 (19)	817.7±18.0 (17)*	874.9±10.8 (21)[a]
Dry HW	mg	DHW	238.3±5.6 (19)	234.8±7.3 (17)	232.9±4.1 (21)
WHW/DHW			3.70±0.04 (19)	3.50±0.04 (17)*	3.77±0.03 (21)[a]

B) Parameter	Unit	NP	P	P0.9
LV diastolic dimensions	cm	0.54±0.04 (7)	0.56±0.06 (6)	0.53±0.02 (10)
LV systolic dimensions	cm	0.28±0.02 (7)	0.33±0.05 (6)	0.26±0.01 (10)
LV shortening fraction	%	47.9±3.3 (7)	41.3±4.2 (6)	50.2±1.7 (10)[a]
LV wall thickness	mm	86±17 (7)	130±15 (6)*	120±20 (10)

(A) Body and heart weights were measured. DHW is determined after an overnight drying at 100 °C. (B) Echocardiography measurements in anesthetized rats. Data are presented as means±S.E.M. (number of animals).

[a] $p<0.05$ vs. P using an ANOVA.

* $p<0.05$ vs. NP using an ANOVA.

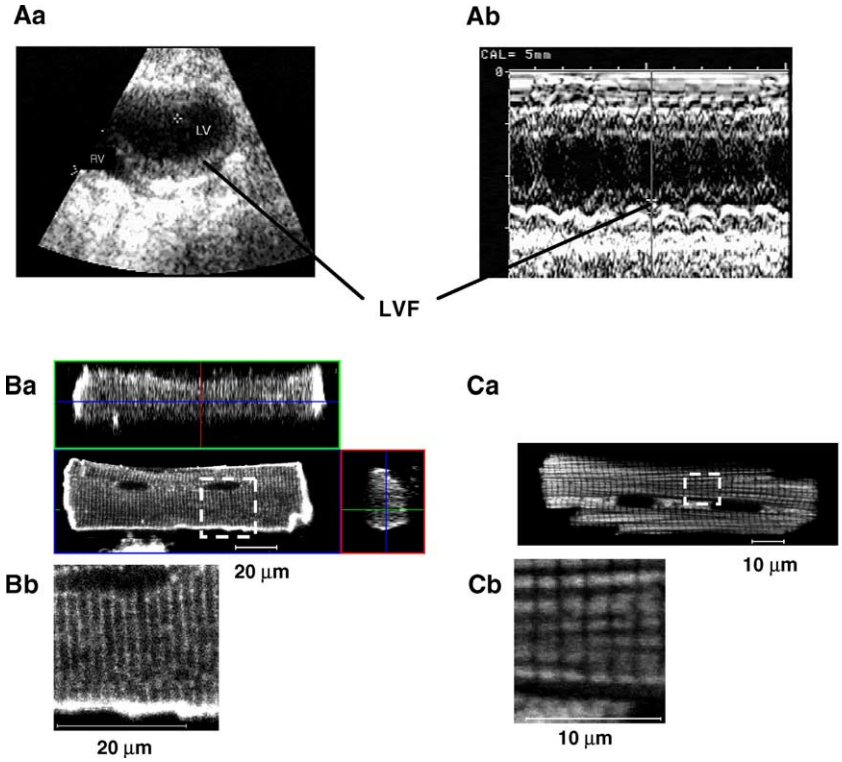

Fig. 1. Myocardial and cardiomyocyte structure. (A) 2D echocardiography picture of a non-pregnant rat heart (Aa). M-mode tracing of the ventricular free-wall movement (Ab). LV: left ventricle, RV: right ventricle, LVF: left ventricular free-wall. (B) 3D representation of an isolated cardiomyocyte loaded with di-8-Anepps (Ba) and detail depicting t-tubular network (Bb). (C) Distribution of mitochondria in single cardiomyocytes imaged using TMRM (Ca) and detail illustrating longitudinally positioned mitochondria (Cb).

rizes data on the cell morphology. In P, we found significant cell elongation due to adding sarcomeres in series when compared to NP. The cross-sectional area (CSA) was consequently increased with the cell volume (geometrical approximation of a cell as an elliptic cylinder [20]: see legend of Table 2), but the length/width ratio was preserved. On the other hand, in P0.9, we identified a different structural remodeling compared to P. Our data revealed further cell enlargement leading to a significantly increased length/width ratio. Interestingly, cells tend to become thinner, allowing preservation of the cell volume. Identical diet given to non-pregnant rats had no significant effect on cell morphology (data not shown).

The length of one individual sarcomere (l_s), a contractile unit of cardiomyocyte, was also established from high precision images of di-8-Anepps stained cells (Fig. 1Bb). In NP, P and P0.9, the t-tubular spacing was estimated to 1.8 µm (Table 2), in accordance with others [21]. Length and area of longitudinally positioned mitochondria were evaluated using TMRM (Fig. 1Ca and Cb). No significant

Table 2
Single cardiomyocyte morphology

Parameter	Unit	ABB	NP	P	P0.9
Cell length	µm	l	113.4±0.8 (406)	117.5±1.1 (250)**	121.2±1.3 (185)[a]
Cell width	µm	w	28.9±0.4 (395)	29.6±0.5 (248)	28.3±0.5 (186)
Cell depths	µm	d	17.6±0.4 (97)	17.8±0.4 (89)	16.5±0.4 (88)
Volume	pL	Vol	43.5±1.3 (97)	48.1±1.8 (89)*	42.6±1.4 (88)
Cross-sectional area	µm^2	CSA	378±10 (95)	415±16 (89)*	350±10 (88)[a]
Length/width		l/w	4.19±0.06 (394)	4.21±0.08 (248)	4.56±0.10 (185)[a]
Sarcomere length	µm	l_s	1.8±0.05 (58)	1.8±0.05 (54)	1.8±0.05 (87)
Sarcomere number		N_s	62±1 (58)	66±1 (54)*	67±1 (87)
Mitochondrial length	µm		1.3±0.1 (14)	1.3±0.1 (12)	1.2±0.1 (6)
Mitochondrial area	µm^2		0.7±0.1 (14)	0.6±0.1 (12)	0.6±0.1 (6)
Membrane capacitance	pF		134.8±4.6 (82)	137.8±5.1 (59)	154.9±6.4 (30)[a]

Comparison of single cell morphology in cardiomyocytes: Vol=$l*w*d*\pi/4$, CSA=$w*d*\pi/4$, $N_s=l/l_s$; mean±S.E.M. (number of cells).
[a] $p<0.01$ vs. P using an ANOVA.
* $p<0.05$ vs. NP using an ANOVA.
** $p<0.01$ vs. NP using an ANOVA.

differences were found in the morphology of mitochondria within the limits of the confocal resolution, suggesting their preservation in all studied conditions. Membrane capacitance, an indicator of the total cell membrane surface, was also determined in pF as an integral of capacitive transients, triggered by hyperpolarizing voltage pulses from holding potential (H.P.) −40 mV to −50 mV, divided by the applied voltage step (10 mV). This overall membrane surface was preserved in P (Table 2), but was significantly increased in P0.9.

3.3. Cardiomyocyte functions

Contractility, the principal function of cardiomyocytes, was questioned using line-scan mode of confocal imaging (Fig. 2Aa) in response to field stimulation at frequency 0.5 Hz (to stabilize SR loading; Fig. 2Ab) and 6 Hz (normal heart rate of NP female rats [19]; Fig. 2Ac). In standard, glucose-based external solution, our results showed that percentage of change in cell length, an index of contractility, was significantly decreased in cells from P in response to stimulation at 0.5 Hz (Fig. 2Ba), as well as 6.0 Hz (Fig. 2Bb), indicating that this effect is not frequency-dependent. In cells from P0.9, the contractility was not significantly different when compared to P. Furthermore, no significant change in cardiomyocyte contractility was observed in NP0.9 (data not shown). Action potentials were not significantly modified in P or P0.9 (data not shown), although some tendency towards AP prolongation was noted in P0.9.

L-type Ca^{2+}currents ($I_{Ca}L$) were also isolated in Cs-based solutions, applying voltage steps of 600 ms from a holding potential of −40 mV every 5 mV at a frequency 0.5 Hz (see inset of Fig. 3Aa for voltage protocol). Our data revealed no significant difference in the current/voltage relationship of the $I_{Ca}L$ density (Fig. 3Ab), expressed as pA/pF, or its activation/inactivation properties (Fig. 3Ac) between P and NP rats. In P0.9, neither $I_{Ca}L$ density nor activation kinetics were significantly modified, but inactivation curve was shifted towards more positive potentials, suggesting larger window current in this condition.

3.4. Metabolic changes

Pregnancy is associated with significant physiologic changes in carbohydrate metabolism [22] to allow continuous nutrients availability to the developing fetus, primarily depending on glucose. We first compared blood levels of glucose, lactate, pyruvate and triglycerides in the different conditions in fed state (Table 3). In P, there was a significant decrease in glycemia, in accordance with glucose being used by the fetus. There was also a significant increase in the levels of triglycerides and lactate with a similar trend on pyruvate, which leads to a significant change in the lactate/pyruvate ratio, indicating an important modification of the redox status. In P0.9, compared to P, neither levels of glucose nor lactate and pyruvate were significantly different, but the lactate/pyruvate ratio failed to increase. These results confirmed changes in the metabolite blood levels during pregnancy.

To question whether described differences are translated into differential use of metabolic reserves by cardiomyocytes in pregnant rats, we tested whether contractility is modified when the cell is exposed, additionally to glucose, to plasma levels of lactate and pyruvate or fatty acid. Cell shortening was assessed in standard external solution

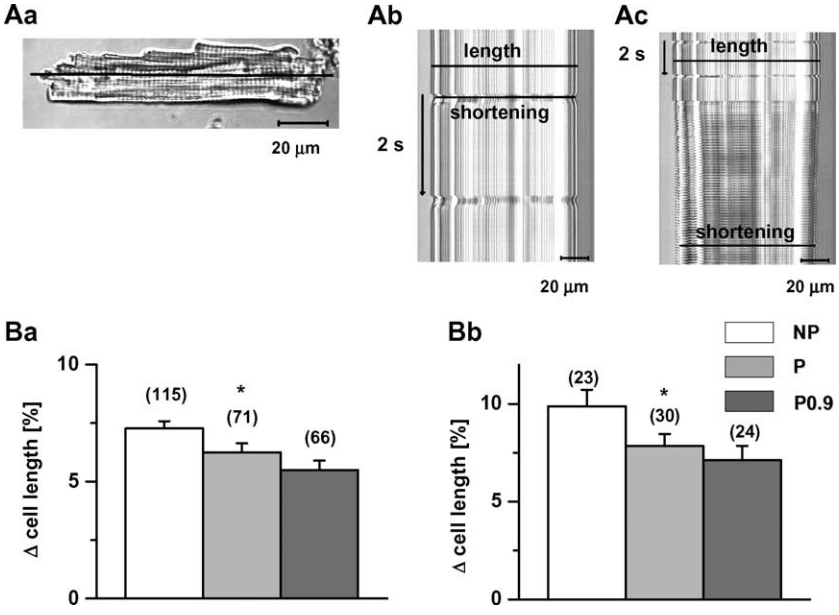

Fig. 2. Single cardiomyocyte contractions. (A) Example of line-scan-imaged cell contractions induced by field-stimulation in a cardiomyocyte (Aa) at 0.5 Hz (Ab) and 6.0 Hz (Ac). (B) Percentage of change in cell length compared at 0.5 Hz (Ba) and 6 Hz (Bb) in basic external solution; mean±S.E.M. (number of cells); *$p<0.05$ using an ANOVA.

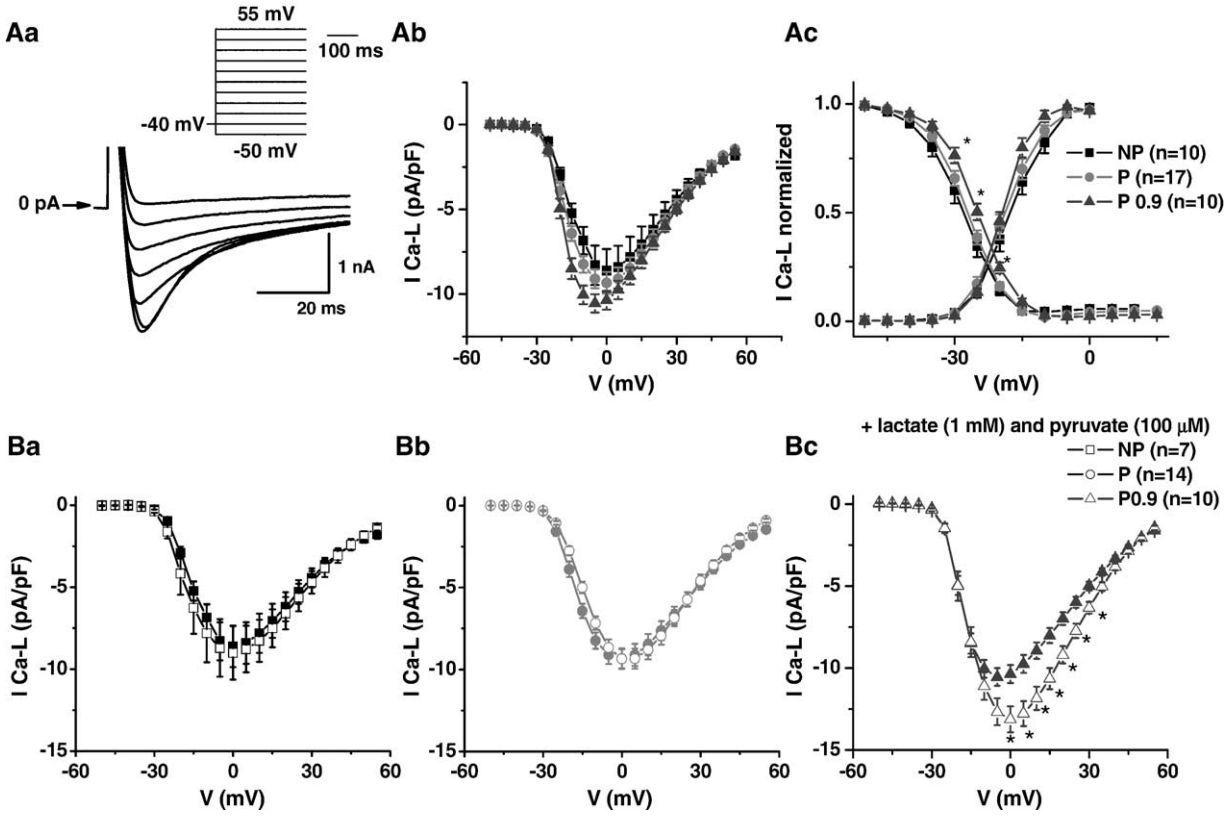

Fig. 3. L-type calcium currents. (A) Example of original recording of L-type calcium current recorded at 35±1 °C using 600 ms voltage pulses, applied from −50 mV to +55 mV from H.P. −40 mV by an increment of 5 mV at a frequency 0.5 Hz with voltage protocol in the inset (Aa). *I*/*V* relationship of $I_{Ca}L$ density, obtained as a difference between peak and end pulse current values (Ab) and its activation and inactivation (at 0 mV) curves (Ac). (B) Effect of 100 μmol/L pyruvate and 1 mmol/L lactate on $I_{Ca}L$ in NP (Ba), P (Bb) and P0.9 (Bc); *$p<0.05$ using an ANOVA.

supplemented with lactate (1 mmol/L) and pyruvate (0.1 mmol/L) or octanoate (1 mmol/L), a medium chain fatty acid. Fig. 4A shows that, in the NP condition, the cell response was not significantly modified by the addition of lactate/pyruvate, whereas when considering pregnancy (P and P0.9), the addition of these substrates significantly increased cell shortening compared to the condition with glucose only. Interestingly, octanoate had a significant effect in NP, but not in P conditions. In P0.9, the effect of lactate/pyruvate was still present, but significantly blunted, while the sensitivity to octanoate was restored. In general, the responsiveness in P0.9 was significantly different from those in P conditions. The pattern of the response was the same at 6 Hz (Fig. 4B), showing that this phenomenon was not frequency-dependent. Furthermore, cells from NP and NP0.9 showed same responsiveness (data not shown). Interestingly, lactate and pyruvate did not affect $I_{Ca}L$ in NP (Fig. 3Ba) or P (Fig. 3Bb), but significantly increased $I_{Ca}L$ amplitude in P0.9 (Fig. 3Bc). Activation/inactivation properties of $I_{Ca}L$ were not modified by these metabolites in either condition (data not shown).

Table 3
Blood metabolite concentrations

Parameter	Unit	NP	P	P0.9
Glucose	mmol/L	16.2±0.8 (5)	9.0±1.4 (5)**	7.6±0.9 (5)
Lactate	mmol/L	1.22±0.04 (5)	2.71±0.27 (5)**	2.26±0.26 (5)
Pyruvate	μmol/L	68.3±9.0 (5)	103.3±8.2 (5)	116.0±18.8 (5)
Lactate/pyruvate		18.8±1.8 (5)	26.4±1.9 (5)*	20.3±1.4 (5)[a]
Triglycerides	mmol/L	1.35±0.25 (5)	3.32±0.66 (5)*	3.40±0.35 (5)

Blood metabolites obtained from total blood collected in fed state; mean±S.E.M. (number of samples).
[a] $p<0.05$ vs. P using an ANOVA.
* $p<0.05$ vs. NP using an ANOVA.
** $p<0.001$ vs. NP using an ANOVA.

4. Discussion

The major findings of our experiments were: (1) an adaptive remodeling of cardiomyocytes is put in place in normal pregnancy, while maladaptive components are identified after sodium supplementation; (2) an adaptation in the utilization of energy substrates is taking place in normal pregnancy and this process is impaired by sodium supplementation, where it involves regulation of $I_{Ca}L$.

4.1. Morphological remodeling in pregnancy

Our first goal in understanding the modifications of LV cardiomyocyte remodeling in normal pregnancy and in the model of experimental preeclampsia was to characterize their structural changes. Morphological parameters gathered

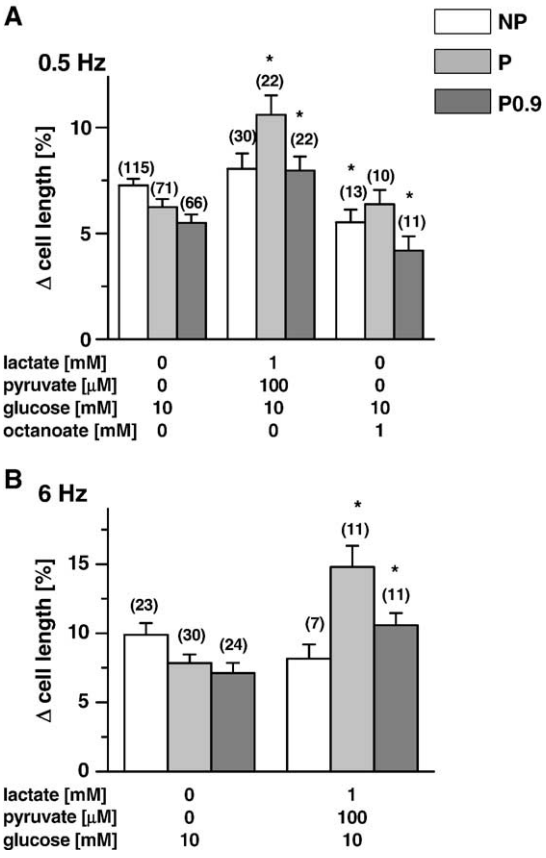

Fig. 4. Effect of metabolite changes on single cell contractility. Cell contractility assessed at (A) 0.5 Hz or (B) 6 Hz in the presence of 1 mmol/L lactate, 100 μmol/L pyruvate or 1 mmol/L octanoate in basic external solution; mean±S.E.M. (number of cells); *$p<0.05$ using an ANOVA.

in non-pregnant rats were in good agreement with others [21,23]. In normal pregnancy, our data identified significantly increased cell length due to adding sarcomeres in series, leading to enhanced cell volume and cross-sectional area. Observed modifications are smaller in comparison to diseased cases [21,24], but are comparable to effects induced by endurance exercise [25]. The length/width ratio and overall membrane surface are preserved in normal pregnancy, according to a proportional myocyte growth observed during volume overload [26]. These results suggest an adaptive cardiomyocyte remodeling, possibly as a result of enhanced volume load placed on the heart. The remodeling of the heart observed during pregnancy resembles the one recorded in women following endurance exercise [27,28], except for hormonal levels.

On the other hand, in experimental preeclampsia, we identified differences in morphological remodeling compared to normal pregnancy. Our results revealed disproportionate cell enlargement in this condition leading to significantly increased length/width ratio, indicating maladaptions [26,29]. Interestingly, to allow preservation of the cell volume, cells tend to become thinner; increase in the cell length rather than CSA was proposed to maintain better diffusion capacities in the heart [26]. Higher membrane capacitance without change in the cell volume in P0.9 suggests bigger dependence of the overall membrane area on cell length, rather than on CSA. This is translated into an increased conversion factor, pointing to disproportionate rise in the t-tubular surface area inside cardiomyocytes [30]. Morphological remodeling observed in this model of experimental preeclampsia therefore shows maladaptive components. A failure to induce adaptive remodeling is likely to result from increased wall stress, triggered by enhanced BP, which is significantly elevated in the animals supplemented with sodium when compared to normally pregnant ones [15].

To understand repercussions of cardiomyocyte remodeling at the whole heart level, we analyzed several cardiac parameters. Observed increase in LV wall thickness in normal pregnancy is in accordance with rise in cardiomyocyte CSA. These results are in agreement with findings in pregnant women [31] that also showed increased wall thickness rather than of LV dimensions. Not significantly modified LV dimensions indicate that induced cellular changes are small, possibly reflecting cardiac adaptations. The very comparable dry weights point to similar levels of myocardial protein contents in all studied groups, in agreement with findings of our colleagues who found no change in LV mass in P vs. NP rats [32]. These data, together with significant change in heart's wet weights in P, when compared to NP condition, indicate that observed changes could be a result of modifications in water retention [33], or increase in the ejection volume. In P0.9, the significant increase in WHWs compared to P, but their similarity with NP indicates a failure to adapt to changes in water retention in this group. This hypothesis is also strengthened by observed cell prolongation, but without significant modifications in LV dimensions.

Enumerated findings in normal pregnancy are in favor with the process of remodeling put in place as an adaptive mechanism to account for hemodynamic changes. On the other hand, sodium supplementation alters this adaptive response and maladaptive components are observed, possibly in reaction to acute pressure overload and/or failure in water retention management, with for probable functional benefits the lowering of wall stress.

4.2. Functional changes

Cardiomyocyte contraction is a hallmark of cellular remodeling and its modifications are often the primary cause underlying changes of the heart function. For these reasons, we investigated whether cardiomyocyte contractile properties are modified in normal pregnancy and whether this homeostasis is altered in experimental preeclampsia. Our results showed that, in glucose-based solutions, the contractility is significantly lowered in cells from P in response to both stimulation frequencies, indicating its frequency-independence. However, in the presence of metabolic substrates, the contractility is increased, suggest-

ing possible compensatory effect. Indeed, fractional shortening of the heart is not significantly modified in P, although it is showing a decreasing tendency. Obtained data are in agreement with somewhat controversial findings of preserved heart contractility in normal pregnancy, reported by some [4,31] and reversible decrease, observed by others [3,34]. In P0.9, we noted a disconnection between fractional shortening and cardiomyocyte contractility suggesting that increase in contractile properties of the heart in this condition are due to changes in loading, metabolic and/or hormonal conditions rather than inotropic state.

Myocardial L-type Ca^{2+} channels are particularly important in triggering cardiomyocyte contractions and therefore we investigated their implication in pregnancy. However, our data indicate that $I_{Ca}L$ is not likely to be responsible for described contractility changes in normal pregnancy, although some possible effects may have been masked by the presence of BAPTA in recorded cells. At the same time, our findings also indicate that the regulation of this current plays a role in the effect of energy substrates on contractility in experimental preeclampsia. Nevertheless, further studies are needed to better understand consequences of metabolic-driven $I_{Ca}L$ changes on excitation–contraction coupling, as well as the role of other ionic currents in the pregnancy-related remodeling. We propose that observed pregnancy-induced cardiac modifications result from combination of load-dependent and heart-rate-dependent changes, with likely implication of hormonal, namely estrogen and/or adrenergic, regulation. Nonetheless, our data also revealed an important contribution of metabolic substrates.

4.3. Metabolic remodeling

Pregnancy is well known to be associated with significant changes in carbohydrate metabolism [22]: glucose homeostasis is affected due to increased fetal glucose uptake. This leads in a more rapid conversion from predominantly carbohydrate to predominantly fat utilization because of earlier depletion of liver glycogen stores, associated with increased lactate and pyruvate levels. Such metabolic changes are also likely to affect heart function. Our data confirmed that, as observed in humans [22], late pregnancy in rats is associated with low blood glucose concentration and increased levels of triglycerides and lactate in fed state. Interestingly, the lactate/pyruvate ratio is also enhanced from physiological values (below 20) to 24, suggesting an effect on redox status. Our results indicate that, in normal pregnancy, cell contractility is more dependent on lactate/pyruvate than in NP condition, but this effect does not require change in $I_{Ca}L$. This dependence on lactate/pyruvate is present, but significantly blunted by sodium supplementation and, in contrast to normal pregnancy, this remaining effect involves increase in $I_{Ca}L$ amplitude. We also investigated the action of fatty acids and we used the medium chain fatty acid octanoate, well used by cardiomyocytes as energy substrate, which oxidation (unlike physiological long chain fatty acids) is not regulated by the carnitine-palmitoyl-transferase 1 (CPT-1) [35]. Octanoate reduced contractility in NP, but not in P although, interestingly, the decrease in contractions could be observed in P0.9. These results suggest that fatty acids are likely to contribute to the metabolic remodeling during pregnancy. Several cardiovascular diseases have been associated with metabolic switches in the fuel partitioning for energy production, but very little is known about cardiac fuel partitioning in pregnancy. In late pregnancy, Sugden and Holness [36] showed a 35% decrease in glucose uptake/phosphorylation by the heart in fed state. Our results suggest that metabolic switch from main substrates glucose/fatty acids to lactate/pyruvate occur in normal pregnancy and that this change has functional consequences on cell contractile properties. Importantly, this adaptation seems blunted by sodium supplementation, where it requires calcium channel regulation.

4.4. Conclusion

Our results shed a new light on mechanisms underlying cardiac remodeling in pregnancy. To our knowledge, this is one of the first studies investigating changes during pregnancy at a single cell level in such details. Our data are in favor with the process of an adaptive cardiomyocyte remodeling in normal pregnancy, while maladaptive components are identified in experimental preeclampsia. Interestingly, the overall different remodeling that is put in place in experimental preeclampsia seems to result from lack of adaptations observed in healthy pregnant rats. Knowledge of cardiovascular adaptations during pregnancy is essential in understanding how these modifications affect the natural course of heart disease and its management during pregnancy.

Acknowledgements

AC is a FRSQ (N° 2948) fellow supported by CFI (N° 9684) and CIHR (MOP 74600). VB-C is recipient of studentship from Foundation of Sainte-Justine Hospital. We would like to thank E. De Smet for helping with some experiments.

References

[1] Jensen E, Wood C, Keller-Wood M. The normal increase in adrenal secretion during pregnancy contributes to maternal volume expansion and fetal homeostasis. J Soc Gynecol Investig 2002;9:362–71.
[2] Schannwell CM, Zimmermann T, Schneppenheim M, Plehn G, Marx BE, Strauer BE. Left ventricular hypertrophy and diastolic dysfunction in healthy pregnant women. Cardiology 2002;97:73–8.
[3] Robson SC, Hunter S, Boys RJ, Dunlop W. Serial study of factors influencing changes in cardiac output during human pregnancy. Am J Physiol 1989;256:H1060–65.

[4] Katz R, Karliner JS, Resnik R. Effects of a natural volume overload state (pregnancy) on left ventricular performance in normal human subjects. Circulation 1978;58:434–41.
[5] Granger JP, Alexander BT, Bennett WA, Khalil RA. Pathophysiology of pregnancy-induced hypertension. Am J Hypertens 2001; 14:178S–85S.
[6] Vazquez BM, Roisinblit J, Grosso O, Rodriguez G, Robert S, Berensztein CS, et al. Left ventricular function impairment in pregnancy-induced hypertension. Am J Hypertens 2001;14:271–5.
[7] Escudero EM, Favaloro LE, Moreira C, Plastino JA, Pisano O. Study of the left ventricular function in pregnancy-induced hypertension. Clin Cardiol 1988;11:329–33.
[8] Novelli GP, Valensise H, Vasapollo B, Larciprete G, Altomare F, Di Pierro G, et al. Left ventricular concentric geometry as a risk factor in gestational hypertension. Hypertension 2003;41:469–75.
[9] Vazquez BM, Grosso O, Bellido CA, Iavicoli OR, Berensztein CS, Vega HR, et al. Left ventricular geometry in pregnancy-induced hypertension. Am J Hypertens 2000;13:226–30.
[10] Valensise H, Novelli GP, Vasapollo B, Di Ruzza G, Romanini ME, Marchei M, et al. Maternal diastolic dysfunction and left ventricular geometry in gestational hypertension. Hypertension 2001;37: 1209–15.
[11] Roy-Clavel E, Picard S, St Louis J, Brochu M. Induction of intrauterine growth restriction with a low-sodium diet fed to pregnant rats. Am J Obstet Gynecol 1999;180:608–13.
[12] Barron WM. Volume homeostasis during pregnancy in the rat. Am J Kidney Dis 1987;9:296–302.
[13] Duvekot JJ, Peeters LL. Renal hemodynamics and volume homeostasis in pregnancy. Obstet Gynecol Surv 1994;49:830–9.
[14] Auger K, Beausejour A, Brochu M, St Louis J. Increased Na+ intake during gestation in rats is associated with enhanced vascular reactivity and alterations of K^+ and Ca^{2+} function. Am J Physiol Heart Circ Physiol 2004;287:H1848–56.
[15] Beausejour A, Auger K, St Louis J, Brochu M. High-sodium intake prevents pregnancy-induced decrease of blood pressure in the rat. Am J Physiol Heart Circ Physiol 2003;285:H375–83.
[16] Battista MC, Calvo E, Chorvatova A, Comte B, Corbeil J, Brochu M. Intra-uterine growth restriction and the programming of left ventricular remodelling in female rats. J Physiol 2005; 565:197–205.
[17] Kawai M, Hussain M, Orchard CH. Excitation–contraction coupling in rat ventricular myocytes after formamide-induced detubulation. Am J Physiol 1999;277:H603–9.
[18] Williamson DH, Mellanby J. Methods in Enzymatic Analysis. NY: Academic Press; 1974: 1836–43pp.
[19] Massicotte G, St Louis J, Schiffrin EL. Heart rate reflex responses during gestation in normotensive and spontaneously hypertensive rats following angiotensin II and vasopressin. Proc Soc Exp Biol Med 1987;186:294–8.
[20] Gerdes AM, Kellerman SE, Malec KB, Schocken DD. Transverse shape characteristics of cardiac myocytes from rats and humans. Cardioscience 1994;5:31–6.
[21] McCrossan ZA, Billeter R, White E. Transmural changes in size, contractile and electrical properties of SHR left ventricular myocytes during compensated hypertrophy. Cardiovasc Res 2004;63:283–92.
[22] Leturque A, Hauguel S, Revelli JP, Burnol AF, Kande J, Girard J. Fetal glucose utilization in response to maternal starvation and acute hyperketonemia. Am J Physiol 1989;256:E699–03.
[23] Satoh H, Delbridge LM, Blatter LA, Bers DM. Surface:volume relationship in cardiac myocytes studied with confocal microscopy and membrane capacitance measurements: species-dependence and developmental effects. Biophys J 1996;70:1494–1504.
[24] Loennechen JP, Wisloff U, Falck G, Ellingsen O. Effects of cariporide and losartan on hypertrophy, calcium transients, contractility, and gene expression in congestive heart failure. Circulation 2002;105:1380–6.
[25] Wisloff U, Loennechen JP, Falck G, Beisvag V, Currie S, Smith G, et al. Increased contractility and calcium sensitivity in cardiac myocytes isolated from endurance trained rats. Cardiovasc Res 2001;50:495–508.
[26] Gerdes AM. Cardiac myocyte remodeling in hypertrophy and progression to failure. J Card Fail 2002;8:S264–8.
[27] Ginzton LE, Conant R, Brizendine M, Laks MM. Effect of long-term high intensity aerobic training on left ventricular volume during maximal upright exercise. J Am Coll Cardiol 1989;14:364–71.
[28] Guazzi M, Musante FC, Glassberg HL, Libonati JR. Detection of changes in diastolic function by pulmonary venous flow analysis in women athletes. Am Heart J 2001;141:139–47.
[29] Katz AM. Maladaptive growth in the failing heart: the cardiomyopathy of overload. Cardiovasc Drugs Ther 2002;16:245–9.
[30] Lipp P, Huser J, Pott L, Niggli E. Subcellular properties of triggered Ca^{2+} waves in isolated citrate-loaded guinea-pig atrial myocytes characterized by ratiometric confocal microscopy. J Physiol 1996; 497:599–610.
[31] Simmons LA, Gillin AG, Jeremy RW. Structural and functional changes in left ventricle during normotensive and preeclamptic pregnancy. Am J Physiol Heart Circ Physiol 2002;283:H1627–33.
[32] Simaan M, Cadorette C, Poterek M, St Louis J, Brochu M. Calcium channels contribute to the decrease in blood pressure of pregnant rats. Am J Physiol Heart Circ Physiol 2002;282:H665–71.
[33] Alexander EA, Churchill S, Bengele HH. Renal hemodynamics and volume homeostasis during pregnancy in the rat. Kidney Int 1980; 18:173–8.
[34] Mone SM, Sanders SP, Colan SD. Control mechanisms for physiological hypertrophy of pregnancy. Circulation 1996;94:667–72.
[35] Depre C, Rider MH, Hue L. Mechanisms of control of heart glycolysis. Eur J Biochem 1998;258:277–90.
[36] Sugden MC, Holness MJ. Control of muscle pyruvate oxidation during late pregnancy. FEBS Lett 1993;321:121–6.